



Original Article

# Atorvastatin from target screening attenuates endothelial cell tube formation and migration by regulating urokinase receptor-related signaling pathway and F/G actin

Li Wei <sup>a</sup>, Jin-Shuen Chen <sup>b</sup>, Hsin-Ting Lin <sup>c</sup>, Chung-Ze Wu <sup>d</sup>, Cai-Mei Zheng <sup>e</sup>, Yu-Ching Chang <sup>f</sup>,  
Li-Chien Chang <sup>f</sup>, Yuh-Feng Lin <sup>b,e,g,\*</sup>

<sup>a</sup> Department of Neurosurgery, Wan Fang Hospital, Taipei Medical University, Taipei, Taiwan, ROC

<sup>b</sup> Division of Nephrology, Department of Internal Medicine, Tri-Service General Hospital, Taipei, Taiwan, ROC

<sup>c</sup> Department of Ophthalmology, Tri-Service General Hospital, National Defense Medical Center, Taipei, Taiwan, ROC

<sup>d</sup> Division of Endocrinology and Metabolism, Department of Internal Medicine, Shuang Ho Hospital, Taipei Medical University, Taipei, Taiwan, ROC

<sup>e</sup> Division of Nephrology, Department of Internal Medicine, Shuang Ho Hospital, Taipei Medical University, Taipei, Taiwan, ROC

<sup>f</sup> School of Pharmacy and Graduate Institute Pharmacy, National Defense Medical Center, Taipei, Taiwan

<sup>g</sup> Graduate Institute of Clinical Medicine, College of Medicine, Taipei Medical University, Taipei, Taiwan, ROC

Received November 17, 2015; accepted February 25, 2016

## Abstract

**Background:** Angiogenesis and cytoskeletal transformation are common denominators of many pathological developments. The relationship between angiogenesis, urokinase plasminogen activator receptor (uPAR) signaling pathway, and cytoskeletal transformation is still unknown. In this study, a pGL3-uPAR promoter reporter system combined with Bio-Plex mRNA analysis was established for discovering uPAR modulators to analyze this interconnection.

**Methods:** After screening a set of clinically used drugs, atorvastatin (Ator) was found to significantly affect uPAR expression and its ideal dose, 1  $\mu$ M, was determined for cell study. Mouse endothelial cell (mEC) models, including tube formation for angiogenesis and wound healing assay for migration, were employed to test the effects on angiogenesis and cytoskeletal transformation with (Group Ator) and without (Group C) the treatment of Ator.

**Results:** The mEC tube formation and migration was significantly decreased in Group Ator. Regarding cytoskeleton changes, the ratio of F/G actin by Western blotting and the assembly of F-actin (lamellipodia) by immunofluorescence were attenuated. Furthermore, uPAR and all uPAR-related factors, including integrin  $\alpha 5\beta 3$ , phosphorylated-focal adhesion kinase, and Rac, revealed a significant reduction when compared with Group C.

**Conclusion:** We conclude that close regulatory machinery spans angiogenesis, uPAR signaling, and cytoskeletal transformation, and that uPAR modulator Ator can decrease the reorganization of actin cytoskeleton, which may lead to a new approach in angiogenesis.

Copyright © 2016, the Chinese Medical Association. Published by Elsevier Taiwan LLC. This is an open access article under the CC BY-NC-ND license (<http://creativecommons.org/licenses/by-nc-nd/4.0/>).

**Keywords:** angiogenesis; atorvastatin; cytoskeleton; urokinase receptor

## 1. Introduction

Angiogenesis occurs under many physiological and pathological conditions and is regulated by a tight balance of angiogenic and antiangiogenic factors, which involves a cascade of events including endothelial cell migration. While the cytoskeleton provides the cell structure, shape, and migration, angiogenesis is strongly related to cellular cytoskeleton changes.

Conflicts of interest: The authors declare that they have no conflicts of interest related to the subject matter or materials discussed in this article.

\* Corresponding author. Dr. Yuh-Feng Lin, Division of Nephrology, Department of Internal Medicine, Shuang Ho Hospital, Taipei Medical University, 291, Zhongzheng Road, Zhonghe, New Taipei City 235, Taiwan, ROC.

E-mail address: [linyuf@stmu.edu.tw](mailto:linyuf@stmu.edu.tw) (Y.-F. Lin).

<http://dx.doi.org/10.1016/j.jcma.2016.02.015>

1726-4901/Copyright © 2016, the Chinese Medical Association. Published by Elsevier Taiwan LLC. This is an open access article under the CC BY-NC-ND license (<http://creativecommons.org/licenses/by-nc-nd/4.0/>).

Urokinase-type plasminogen activator receptor (uPAR) is a protein that has been proven to play a major role in the regulation of angiogenesis and cytoskeletal formation. Current evidence from *in vivo* studies suggests that uPAR expression is elevated during inflammation, tissue remodeling, and in many human cancers, and its presence frequently indicates poor prognosis.<sup>1</sup> On the other hand, *in vitro* studies have proved that uPAR regulates proteolysis by binding to extracellular protease uPA, activating many intracellular signaling pathways. Apart from uPA, uPAR also binds to transmembrane protein integrin and initiates the activation of intracellular signaling molecules, such as focal adhesion kinase (FAK), resulting in rearrangements of the actin cytoskeleton and cell movement.<sup>2,3</sup> Many advances have been made since the discovery that uPAR regulates cell signaling independently of uPA-mediated proteolysis. Taken together, uPAR's important function in cell migration, proliferation, and survival involves coordination of extracellular matrix proteolysis, making it an attractive therapeutic target in cancers and inflammatory disorders.

Many efforts are taken to find drugs that modulate the uPA/uPAR signaling system. Several models based on mechanisms affecting uPA–uPAR interaction,<sup>4,5</sup> capturing ligands to scavenge signal transduction,<sup>6,7</sup> and/or inhibiting biosynthesis<sup>8</sup> have been developed. Recent reports suggest that uPAR can be a useful target for the prevention of invasion and metastasis of certain human cancers, and downregulation of uPAR expression by anti-genetic techniques reverses tumor invasive behavior, induces substantial tumor regression, or even totally inhibits tumor metastasis.<sup>9</sup> Since uPAR-null mice were born and survived to adulthood with no overt phenotypic abnormalities, it was proved that this specific gene deletion did not affect normal physical development, normal reproduction, normal thrombosis, and angiogenesis.<sup>10</sup> Thus, we proposed to construct a cell-based luciferase assay system to screen uPAR synthesis inhibitor from clinically used small-molecule drugs to provide alternative treatment modality beyond their present indications. As this system was an *in vitro* study, a secondary assay via determining its mRNA expression by Bio-Plex system was done to synchronize the efficacy of leading drugs discovered by the assay system in our study.

First, a uPAR promoter (uPARp) plasmid was established to screen candidate drugs to determine whether uPAR signaling pathway is needed for endothelial cell migration and tubule angiogenesis and to determine the potential drugs modulating this uPA/uPAR signaling pathway. The aim of our study was to investigate the possible mechanism of uPAR in cytoskeletal transformation and to develop novel treatment modalities for diseases with angiogenesis abnormalities.

## 2. Methods

### 2.1. Experimental design

Two cell lines were used to discover the universal function of the uPAR modulator between strains. HeLa cells were used to establish a reporter system and obtain candidate drugs. Mouse endothelial cell (mEC) models of angiogenesis and

migration were established by tube formation and wound healing assays for *in vitro* studies regarding angiogenesis.

First, a platform of uPARp-luciferase reporter system was established to screen the candidate drugs modulating the uPAR expression. Next, atorvastatin (Ator), which was suggested by the drug screening system, was used to treat mECs (1  $\mu$ M Ator for 8 hours) to evaluate the changes in angiogenesis and migration. Finally, the protein extracted from these two cell models were analyzed for the signaling pathway from uPAR to F-actin assembly by Western Blot (WB) and immunofluorescence (IF) assays. Data were analyzed and discussed after the results.

### 2.2. uPARp-luciferase reporter system

A platform of uPARp-luciferase reporter system was established to screen candidate drugs modulating the expression of uPAR.

#### 2.2.1. Construction of pGL3-uPARp plasmid

The full-length coding region of the responsive element of human uPARp (uPARp-RE;  $-498/+22$ )<sup>11</sup> was derived by polymerase chain reaction (PCR) from genomic DNA of HeLa cells. The PCR amplification was performed with the primers 5'-CGGTACCGTGCTGGGCACTGGTCCAG-3' and 5'-CAAGCTTCTGCACGTCTTCTCTCTCTCTG-3' by a thermal program comprised initial denaturation at 95°C for 5 minutes, 35 cycles of 95°C for 30 seconds (denaturation), 50°C for 30 seconds (annealing), 72°C for 30 seconds (extension), and 72°C for 10 minutes (final extension). Then, the amplified DNA was purified by gel electrophoresis and ligated into pGL3 luciferase reporter plasmid with HindIII and KpnI digestion to prepare the plasmid construct. The success of construction was verified by sequence analysis of the entire enhancer region of the pGL3-uPARp plasmid.

#### 2.2.2. Transient transfections and luciferase activity assays

Since the modulator effect was indexed by the reporter activity of the pGL3-uPARp construct, a transient transfection procedure was performed each time prior to assay. In brief, HeLa cells were harvested at approximately 50% confluence and seeded in six-well dishes at  $5 \times 10^5$  cells/well with Dulbecco's modified Eagle's medium (DMEM) containing 10% fetal bovine serum (FBS). After 24 hours of recovery, cells were treated with a mixture of pGL3-uPARp plasmid and TurboFect reagent (Fermentas, Burlington, Ontario, CA) at a ratio of 1:1.5 to prepare transfected cells, and control cells were those transfected with plasmid only. After 16 hours of exposure, transfected cells were washed twice with DMEM and incubated with medium containing a screening drug (10 M) from a 38-clinical-drugs library. Cells were lysed 24 hours post-transfection and analyzed for the luciferase activity. A duplicate experiment with cotransfection of a constitutively expressed renilla luciferase plasmid was performed to reduce a possible false positive for some hits expressing a prominent change in solo luciferase expression. Luciferase assays were conducted using Dual-Glo Luciferase Assay System (Promega, Madison, WI, USA) and a Tecan

Infinite M200 microplate reader (Tecanm, Männedorf, Switzerland). Results were expressed as relative light units or fold increase versus the control.

### 2.2.3. Multiplex mRNA assay

In order to justify the fidelity of the established drug screening platform transcriptionally, analysis of mRNA expression of these screening cells was also performed. Briefly, total RNA of each sample was isolated using Trizol reagent (Invitrogen, Carlsbad, CA, USA), according to the manufacturer's protocol. Isolated RNA was quantified by UV spectrophotometry and diluted to 1  $\mu\text{g}/\mu\text{L}$  in diethyl pyrocarbonate-treated water for expression analysis. Determination of mRNA expression was performed using the Bio-Plex multiplex suspension assay system (Bio-Rad, Hercules, CA, USA) with GAPDH as an internal control in which individual bead-based oligonucleotide probe sets specific for uPAR and GAPDH were developed using previously published NCBI gene accession numbers. To perform the Bio-Plex assay, 1  $\mu\text{g}$  of total RNA was reverse-transcribed to cDNA using oligo (dT) primers, and the resulting product (1  $\mu\text{L}$ ) was amplified by PCR with biotinylated sequence-specific primers. Then, the amplicons were hybridized with X-MAP beads containing oligonucleotide capture probes at 50°C for 1 hour, followed by incubation with streptavidin-conjugated R-phycoerythrin at 50°C for 30 minutes, and finally subjected to Bio-Plex quantitation. Results were standardized by GAPDH and expressed as the ratio of relative light units of the target mRNAs.

### 2.3. MTT and RNA assays to determine the optimum doses of atorvastatin

To determine the optimum dose of Ator for further study on the effect of angiogenesis and cytoskeletal transformation, we evaluated the cytotoxicity effect of Ator on mECs using an MTT assay. Each assay included Groups Ator and vehicle (i.e., DMSO) only (Group C), and the mECs were treated with various concentrations (i.e., 0.1–10  $\mu\text{M}$ ) of Ator for 24 hours at 37°C according to the protocol previously described.<sup>12</sup> To confirm the consistency of effect of Ator on various uPAR strains, total RNA was extracted using Trizol reagent (Invitrogen) from mECs with/without the treatment of Ator 1  $\mu\text{M}$  for mRNA analysis. The methodology was as previously described,<sup>13</sup> and the forward and reverse primers were 5'-Biotin-GGAAGAACCCATGGGACTC-3' and 5'-TTTG TGGCGCACACGGTCTC-3', respectively. PCR amplification was performed at 94°C for 3 minutes, 94°C for 30 seconds for 35–40 cycles, 50–60°C for 30 seconds, and 72°C for 30 seconds, followed by a final extension at 72°C for 10 minutes. The resulting GAPDH and uPAR gene products were electrophoretically separated on 1% agarose gel and stained with ethidium bromide.

### 2.4. Cell models

#### 2.4.1. Mouse endothelial cell

Mycoplasma-free SV-40 transformed mouse pancreatic islet endothelial cells (American Type Culture Collection, CRL-2280) were purchased from Bioresources Collection and

Research Center, Taipei, Taiwan. All experiments were performed between 30 and 40 generations. The cells were prepared and kept in DMEM with 4 mM L-glutamine, 1.5 g/L sodium bicarbonate, 4.5 g/L glucose, 1.0 mM of sodium pyruvate, and 5% FBS. All the culture media were purchased from GIBCO Life Technology (Thermo Fisher Scientific, Waltham, MA, USA).

#### 2.4.2. Angiogenesis

For angiogenesis assay, tube formation was performed. Tube formation is an easy-to-perform assay based on differentiation of endothelial cells and formation of tube-like structures on an extracellular matrix, Matrigel (BD Biosciences, Franklin Lakes, NJ, USA). It is also called *in vitro* Matrigel Angiogenesis Assay. First, 280  $\mu\text{L}$  of thawed Matrigel solution was added to each well of a pre-chilled 96-well sterile plate. After incubation for 2 hours, Matrigel solution turns to a gel. Then, 250  $\mu\text{L}$  of mEC suspension ( $2 \times 10^5$  cells) per well was added into the solidified Matrigel gel. At the same time, 1  $\mu\text{M}$  Ator was added into the well, which was denoted as the experimental group (Group Ator). The group without the Ator treatment denoted as the control group (Group C). After 8 hours with/without treatment, all cells were stained with hematoxylin and photographed. Images were analyzed in Image J (<http://rsb.info.nih.gov/ij/>) to determine the tube length.

#### 2.4.3. Wound healing assay

For cell migration, mECs were cultured in a six-well plate at a density of  $1 \times 10^6$  cells/well. Groups Ator and C were used for the assay of cell migration, as previously described.<sup>12</sup> Each experiment was performed at least three times independently. For analysis, Image J file was opened at 0 hour and 16 hours, and the rate of wound closure was calculated. Data were expressed as percentage of wound closure relative to width of control wounds photographed at 0 hour. The wound closure area of cells cultured in Group C was set at 100%.

To determine cell migration from rate of cells themselves but not from the rate of cell proliferation, cells from Group Ator were checked with MTT at 0 hour and 16 hours. The growth rate of mECs from 0 hour to 16 hours was calculated. The formula for growth rate is  $16 - 0 \text{ hours} / 0 \text{ hour}$ . Each experiment was performed at least three times independently and used to compare the data of cell migration.

### 2.5. Protein extraction, WB and IF

#### 2.5.1. Protein extraction

Mouse endothelial cells were cultured in 10-cm petri dishes at a density of  $1 \times 10^6$  cells/dish. After 8 hours of treatment with/without the 1  $\mu\text{M}$  Ator, protein was extracted as described previously.<sup>12</sup> Protein concentration was determined using the BCA assay kit (Pierce, Rockford, IL, USA). Samples were stored at  $-70^\circ\text{C}$  until use.

#### 2.5.2. WB analysis

To study the amount of uPAR-related signaling proteins, protein extracts from mECs of Groups Ator and C were subjected to WB, which was performed as previously described.<sup>12</sup>

In brief, all membranes were incubated overnight at 4°C with antibodies against three proteins, active  $\beta_3$  integrin, specific murine monoclonal antibody  $\alpha_5\beta_3$  (AP5) with 1:50 dilution (GTI Diagnostics, Inc., Waukesha, WI, USA), phospho-FAK (Tyr397) with 1:1000 dilution (Cell Signaling Technology, Danvers, MA, USA), and Rac1/2/3 with 1:1000 dilution (Cell Signaling Technology). The next two proteins were incubated at room temperature for 1 hour with uPAR 1:1000 (Santa Cruz Biotechnology, Inc., Santa Cruz, CA, USA), and anti-actin antibody 1:500 (Cytoskeleton Inc., Denver, CO, USA). Subsequently, goat anti-rabbit horseradish-peroxidase (HRP: Jackson ImmunoResearch Laboratories, West Grove, PA, USA) and goat anti-mouse HRP (Santa Cruz, CA, USA)-labeled secondary antibody were used to detect candidate proteins. For densitometry, all results were normalized to actin content and expressed as a ratio compared to that of Group C. Data from three separate experiments were pooled for analysis.

For the F/G-actin ratio, protein extracts from mECs from Groups Ator and C were subjected to an F/G-actin *in vivo* assay kit (Cytoskeleton) based on the manufacturer's protocol and as previously described.<sup>12</sup>

### 2.5.3. IF

IF staining of F-actin for cells indicated the cytoskeletal rearrangement in cells.<sup>14,15</sup> To localize the expression of F-actin, mECs from Groups Ator and C were subjected to IF as previously described.<sup>12</sup> The developed sections were visualized by an optical photomicroscope (Olympus, Tokyo, Japan). Negative controls, from which primary antibodies were omitted, were included in the assay.

To study the expression of uPAR-related signaling factors, particularly in surface proteins, including uPAR and AP5, IF was done. mECs from Groups Ator and C were subjected to IF. The methodology was the same as previously described.<sup>12</sup> Primary antibody for uPAR was 1:50 diluted for 1 hour, and secondary antibody was goat anti-mouse fluorescein isothiocyanate (FITC) which was 1:200 diluted for 1 hour. The primary antibody for AP5 was 1:50 diluted for 1 hour, and secondary antibody was Alexa Fluor 488 which was 1:200 diluted for 1 hour. All developed sections were visualized using an optical photomicroscope (Olympus).

### 2.6. Statistical analysis

All experiments were normalized with controls and compared with Ator and repeated at least three times. Results within groups were expressed as the mean  $\pm$  SEM. Unpaired *t* tests were used to assess the statistical significance of differences between two groups, and paired *t* tests were used for within-group comparisons. A *p* value < 0.05 was considered significant.

## 3. Results

### 3.1. Plasmid reporter system

In the study, we performed a small molecule-based screening using a library of common clinical drugs to discover the

potential uPAR modulators. It aimed to identify targets which, when interacting with the uPARp gene, might have led to the alteration of uPAR expression. A uPARp reporter assay system (Fig. 1A) based on uPARp-RE positioned upstream of the reporter firefly luciferase was constructed firstly to probe the changes in uPAR signal transduction and gene transcription. Using the genetic uPARp-RE-based reporter assay, a small clinical drug library against approximately 38 targets was screened. From the primary screen and retest, 16 drugs were shown to cause >15% variation of the uPAR reporter activity, resulting in a hit rate of 42% (Table 1). While a moderate specificity can be offered by the assay with its dual luciferase format which minimizes the risk of false hits via normalizing uPAR-dependent firefly luciferase activity against the constitutively expressed renilla luciferase activity, the hit rate obtained might be too voluminous to positively point out compounds with uPAR activity. Such a problem might be inherent in complex machineries of uPAR signaling cascade.

### 3.2. Lead compounds transcriptionally verified by Bio-Plex analysis

To further eliminate the compounds that affect the uPARp reporter activity due to incorrect transcriptional/translational machineries, we examined these drugs by a second cell-based assay via determination of uPAR mRNA variation using Bio-Plex technology. The assay helped us exclude compounds that might be general modulators of pGL3-control and pRL-SV40 reporters. After repeated examination, as Table 1 shows, 3 of the 16 hits, including Ator, M1, and M8, were verified to transduce alteration of uPAR expression from promoter to mRNA (>40% variation). Among them, Ator and M8 (an anti-cancer drug) affected uPAR reporter activity and mRNA expression with one accord; however, M1 regulated the promoter activity and mRNA non-synonymously. Given M8 might easily suffer in a false-positive paradigm due to its cytotoxicity, Ator was finally chosen as uPAR modulator for further experiments.

### 3.3. Optimum dose of Ator

Since the readout of reported gene assays tends to be susceptible to certain features inherent to biological mechanisms of genes,<sup>16</sup> the ideal dose of Ator for further cellular studies was investigated in a dose-dependent manner. After treatment with various concentrations of Ator on mECs for 24 hours, as shown in Fig. 2A, the suppression of cell growth was significant (*p* < 0.05) for an Ator concentration above 1  $\mu$ M compared with Group C. At this concentration, the expressions of promoter, mRNA, and protein of uPAR were all significantly decreased (Fig. 2B), which confirmed our findings that Ator is a potent uPAR modulator.

### 3.4. Effect of Ator on *in vitro* endothelial cell tube formation and migration

After treatment with 1  $\mu$ M Ator for 8 hours, *in vitro* mEC angiogenesis and migration were performed. With a further 8-

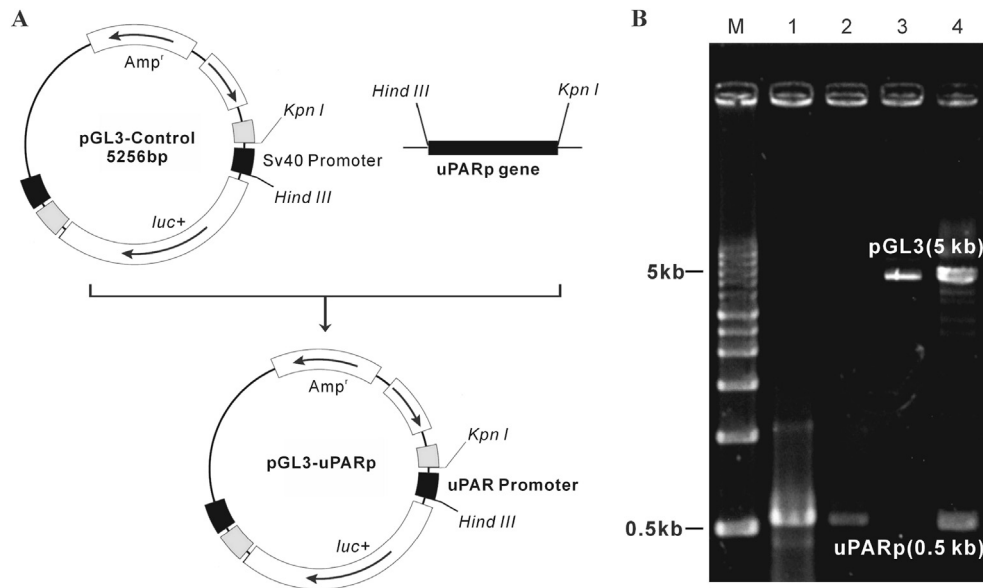


Fig. 1. Construction and restriction analysis of recombinant plasmid pGL3-uPARp. (A) Construction of the recombinant plasmid pGL3-control with uPARp gene. uPARp gene and plasmid pGL3-control DNA were digested by *Kpn*I and *Hind*III and ligated using T4 DNA ligase, yielding recombinant plasmid (pGL3-uPARp) with a *Amp*<sup>r</sup> gene as a selection marker. (B) Restriction analysis of the recombinant plasmid pGL3-uPARp. M, marker; lane 1, PCR product using HeLa cells genomic DNA as template; lane 2, PCR product digested with *Hind*III and *Kpn*I; lane 3, plasmid pGL3 digested with *Hind*III and *Kpn*I; lane 4, pGL3-uPARp digested with *Hind*III and *Kpn*I.

Table 1  
Screening drugs of uPAR expression by luciferase assay and Bio-Plex.

Compounds	uPAR expression		Compounds	uPAR expression	
	Promoter RLU luc/RLU ren	mRNA (uPAR/GAPDH)		Promoter RLU luc/RLU ren	mRNA (uPAR/GAPDH)
Aspirin	1.23 <sup>a</sup>	1.03	L1	1.14	0.94
<b>Atorvastatin</b>	<b>1.37<sup>a</sup></b>	<b>1.43<sup>b</sup></b>	M1	0.85 <sup>a</sup>	1.59 <sup>b</sup>
B4	0.94	0.94	M8	1.31 <sup>a</sup>	1.49 <sup>b</sup>
B5	1.06	1.05	O1	0.94	1.05
B9	0.91	0.89	O2	1.13	0.93
B11	0.74 <sup>a</sup>	0.92	P7	1.14	0.96
B13	0.85 <sup>a</sup>	0.97	Q1	1.08	1.06
C6	1.24 <sup>a</sup>	1.19	Q2	1.66 <sup>a</sup>	1.17
C8	1.10	1.01	R 1	1.10	1.05
D13	0.76 <sup>a</sup>	0.94	R2	1.02	0.89
E0	0.77 <sup>a</sup>	0.88	S0	1.05	1.28
E7	1.10	1.20	S1	1.18 <sup>a</sup>	0.77
G1	0.76 <sup>a</sup>	1.03	S9	1.11	0.81
G6	0.94	0.86	S11	0.98	0.78
H1	1.26 <sup>a</sup>	0.69	S13	1.00	1.08
H2	1.22 <sup>a</sup>	0.81	T12	1.01	0.90
H3	1.13	0.99	T13	1.18 <sup>a</sup>	1.07
H5	1.11	0.76	V1	1.14	0.96
K1	1.13	0.99	Z1	0.84 <sup>a</sup>	0.90

uPAR, urokinase plasminogen activator receptor; mRNA, messenger RNA; RLU luc, relative light unit of firefly luciferase; RLU ren, relative light units of renilla luciferase; GAPDH, glyceraldehyde-3-phosphate dehydrogenase.

<sup>a</sup> Compared to control, >15% variation.

<sup>b</sup> Compared to control, >40% variation.

hour observation, tube formation in Group Ator was statistically decreased compared with that in Group C based on triplicate experiments (Fig. 3A). Regarding cell migration, a scratch wound was created, and subsequent observation was conducted for 16 hours. At 16th hour, the ability of wound closure was significantly decreased in Group Ator compared with Group C

(Fig. 3B). The data of cell proliferation showed insignificant differences among the two groups (data not shown) at 16 hours of observation. The rate of mEC proliferation was calculated, and no significant changes were noted between 0 hour and 16 hours. Taken together, our findings suggest that Ator decreases mEC migration itself but not due to cell proliferation.

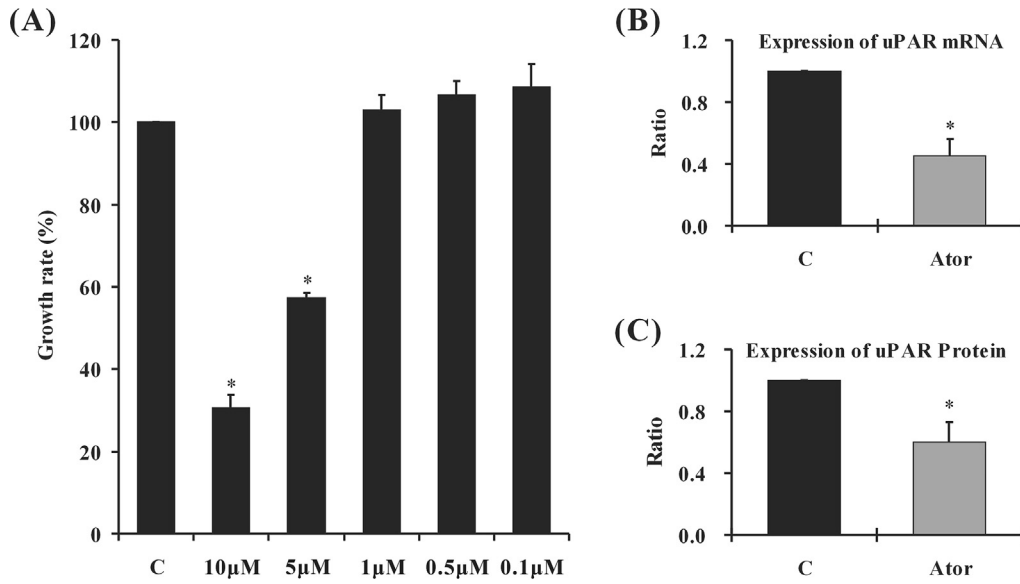


Fig. 2. Determination of ideal dose of atorvastatin (Ator) by MTT assay. (A) X-axis shows different doses of Ator-treated mouse endothelial cells (mECs). Y-axis is percentage of growth rate of mECs. The dose of 1 µM showed a maximum dose without cell cytotoxicity. Subsequently, mECs were treated with 1 µM Ator for 24 hours, and then mECs mRNA and total protein were harvested. (B, C) Show after triplicate experiments, the mRNA and protein expression of uPAR, at 45% and 60%, respectively, is significantly decreased in Group Ator in ratio to Group C. \* $p < 0.05$  versus Group C.

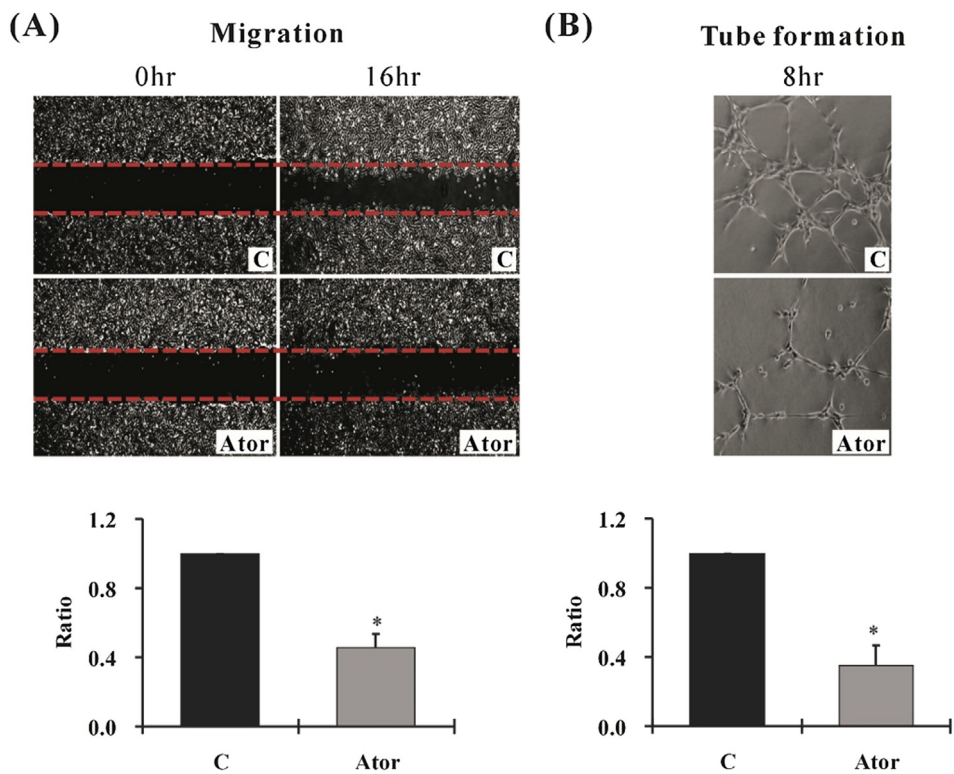


Fig. 3. Effect of 1 µM atorvastatin (Ator) on mouse endothelial cell tube formation and migration. Mouse endothelial cells were treated (Group Ator) or not treated (Group C) by Ator for 8 hours, and then after a further 16 hours and 8 hours, wound healing assay and tube formation were analyzed, respectively. (A) A representative picture of tube formation at 8 hours. After triplicate experiments, the ability of tube formation in Group Ator is 35% in ratio to that of Group C. (B) A representative picture of wound healing assay at 16 hours. After triplicate experiments, the ability of migration in Group Ator is 45% in ratio to that of Group C. \* $p < 0.05$  versus Group C.

### 3.5. Effect of Ator on uPAR-related signaling factors at the cellular level

Regarding the uPAR-related signaling factors, uPAR, AP-5, p-FAK, and Rac were enrolled. After 8 hours of treatment with 1  $\mu\text{M}$  Ator, mECs were harvested to investigate the expression of uPAR-related signaling factors by WB and IF. As Fig. 4A–C reveal, the amount of all proteins, uPAR, AP5, p-FAK, and Rac reduced significantly in Group Ator compared with Group C. Among them, two membrane proteins, including uPAR and AP5, were stained by IF. The intensity of these two proteins also was weaker in Group Ator than in Group C. Taken together, all uPAR-related signaling factors were decreased after the treatment of Ator.

### 3.6. Effect of Ator on the expression of cell cytoskeleton, F-actin

After 8 hours of treatment with 1  $\mu\text{M}$  Ator, the changes in cytoskeleton of mECs were evaluated by F/G actin ratio and F-actin assembly. First, as seen in Fig. 5A, the F/G actin ratio in Group Ator was decreased significantly compared with that in Group C. Subsequent remodeling of F-actin is shown in Fig. 5B. The assembly of F-actin in Group C was a pattern of lamellipodia; however, after Ator treatment, intensity of lamellipodia became vague. Taken together, our data might suggest that condition of mEC in either decreased F/G actin ratio or F-actin expression in lamellipodia, or both, leads to attenuation of the development of cell migration and tube formation.

## 4. Discussion

Since uPAR was found to play a role in tumor development and progression, a considerable amount of effort has been devoted to identify uPAR inhibitors for cancer therapy. Further, in a previous study, we found that cell migration expression was inhibited after treatment with uPAR antibody under a high temperature of 39°C (data not shown). Although several classes of uPA inhibitors have been developed to exhibit the inhibition of uPA/uPAR pathway *in vitro*, their destiny to pass *in vivo* examinations finally onto market, however, was dismal due to lack of desired pharmacokinetic properties or toxicity profiles.<sup>17</sup> Thus, in a more recent study, we conducted the library screening based on clinically used drugs, which had several advantages over current drug screening programs. First, we used the commonly used drugs with already proven safety and known pharmacokinetic properties. Second, new pathological mechanisms or drug–drug interactions on uPA/uPAR pathway could be identified by this study, thereby expanding the post-marketing drug safety database with knowledge of the uPA/uPAR pathway. Nevertheless, this is the first paper to identify Ator, a lipid-lowering agent, as having an all-around effect on uPA/uPAR-signaling pathway from gene expression, signal transduction, and cytoskeletal transformation to cellular functions.

Reporter assays have been used in numerous pharmacological studies investigating full or partial agonists,

antagonists, or inverse agonist. They are also well suited for high-throughput screening approaches in various assay formats. However, the application of the reporter assay is limited by certain features inherent to the assay itself, especially when the regulatory machineries have evolved in the context of complex responsive elements which behave differently with dose. For example, available data indicates that aspirin upregulates the expression of uPAR gene in human colon cancer cells<sup>18</sup> but inhibits the formation of uPA-uPAR-integrin complexes in highly invasive prostate cancer cells.<sup>19</sup> In one study, the modulatory function of aspirin on uPAR was tested at 10  $\mu\text{M}$  and merely showed that the promoter activity was affected (Table 1). Therefore, it is important to control artifacts that might arise from the biological dose-dependent regulation machinery while using the developed uPAR screening system. In this regard, we verified the modulatory effect of Ator on uPAR with its promoter, mRNA, and protein prior to comprehensive cell studies.

The optimum dose of Ator for endothelial cell *in vitro* study was 1  $\mu\text{M}$  in our study, which was suggested by the MTT assay. According to our previous report,<sup>20</sup> statins are divided into two groups, synthetic and fermentation-derived. For *in vivo* studies, the uptake of statins is determined by lipophilicity. In terms of lipophilic nature, lovastatin and simvastatin are the most lipophilic, followed by Ator, fluvastatin, and pravastatin. Predominantly lipophilic statins penetrate cells to a higher degree than predominantly hydrophilic statins, suggesting that the lipophilicity of statins might determine the experimental dose appropriate for cell studies. Based on the pharmacokinetic characteristic of statins and studies,<sup>21–23</sup> the ideal dose of Ator for endothelial cells is from 500 nM to 10  $\mu\text{M}$  depending on different study design.

The process of angiogenesis includes tube formation and cell migration. In our study, 1  $\mu\text{M}$  Ator attenuated the angiogenesis process via inhibiting tube formation and cell migration. According to Urbich et al,<sup>24</sup> Ator dose-dependently affects human umbilical endothelial cell (HUVEC) migration and angiogenesis. A concentration between 0.01  $\mu\text{M}$  and 0.1  $\mu\text{M}$  promotes HUVEC migration and tube formation. In contrast, a higher concentration (>0.1  $\mu\text{M}$ ) of Ator blocks angiogenesis and migration. In our study, we did not investigate the different doses of Ator with regards to the angiogenesis ability of mECs; however, we confirmed that 1  $\mu\text{M}$  Ator attenuated angiogenesis, similar with the findings of Urbich et al.<sup>24</sup>

In our study, 1  $\mu\text{M}$  Ator attenuated uPAR-related signaling factors, including uPAR, AP5, p-FAK, and Rac. The relationship between uPAR-related signaling factors and Ator has been suggested by evidence, but most studies have only shown uPAR with one or two factors and not all four factors as in our study. Stach et al<sup>21</sup> suggested the 1  $\mu\text{M}$  Ator reduces the expression of uPAR on HUVEC surface by flow cytometry. Kawakam et al<sup>25</sup> suggested that Ator inhibits the activation of FAK in U937 cells. As for integrin, integrins are obligate heterodimers containing two distinct chains called  $\alpha$  and  $\beta$  subunits. In mammals, 18  $\alpha$  and 8  $\beta$  subunits have been described. The  $\alpha$  and  $\beta$  subunits each penetrate the plasma

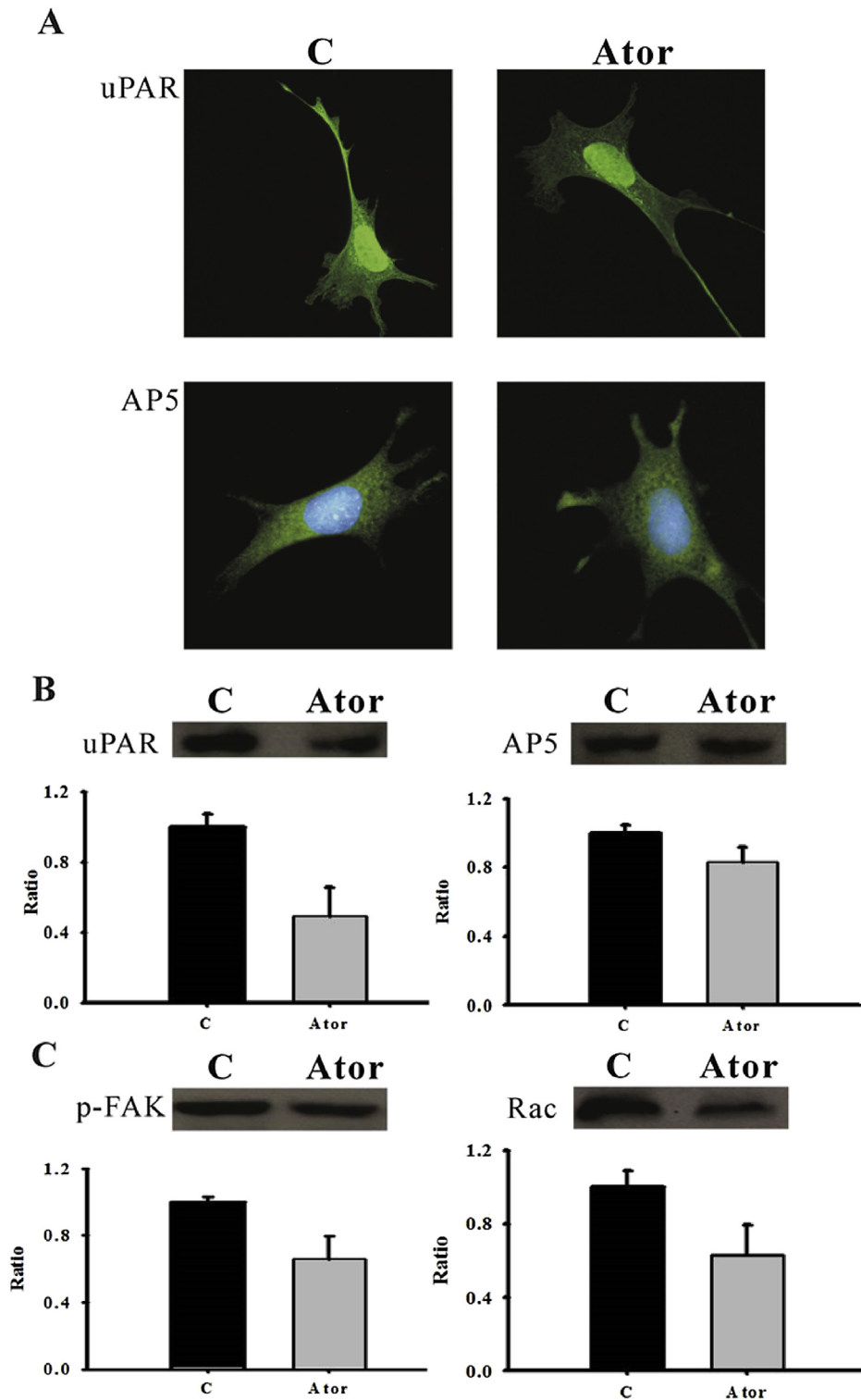


Fig. 4. Expression of urokinase plasminogen activator receptor (uPAR)-related signaling factors at cellular level. Mouse endothelial cells were treated by 1  $\mu$ M atorvastatin (Ator) for 8 hours (Group Ator), and then cells were harvested for immunofluorescence (IF) and Western blot (WB). uPAR and integrin  $\alpha 5\beta 3$  (AP5) were analyzed by WB and IF as (A) and (B) show; however, phosphorylated-focal adhesion kinase (p-FAK) and Rac were analyzed by WB alone as (C) shows. In the IF expression of uPAR (green) and AP5 (green), the intensity of IF in Group Ator is significantly weaker than that of Group C. This finding was confirmed by WB as (B) shows. As for the protein amount of uPAR, AP5, p-FAK, and Rac, all results for densitometry were normalized to actin content and expressed as a ratio compared to that of Group C. Data from three separate experiments were pooled for analysis. Representative plots (B, C) show the protein expression of uPAR, AP5, p-FAK, and Rac, and all statistical data in Group Ator are lower than that of Group C.



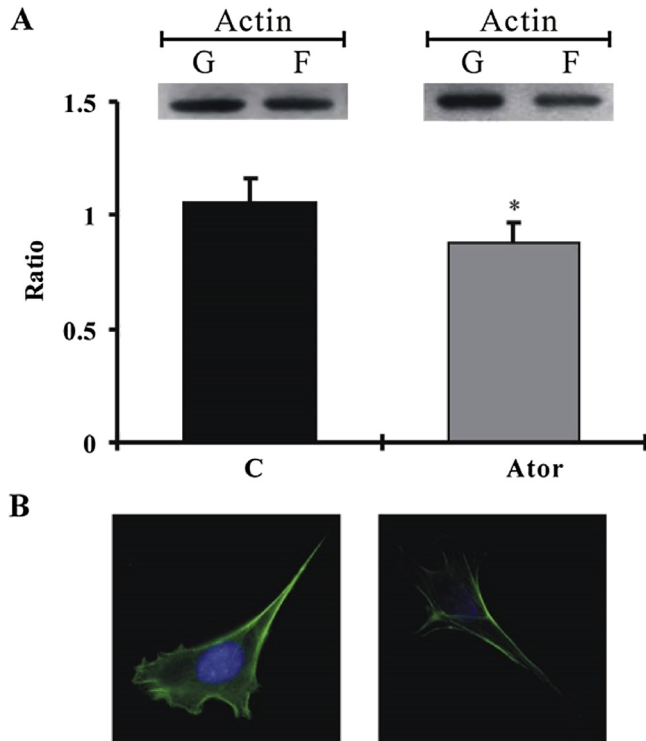


Fig. 5. Ratio of F/G actin and assembly of F-actin with/without the treatment of atorvastatin (Ator) at cellular level. Assembly of F-actin was evaluated by immunofluorescence. (A) The expression of F- and G-actins responding to the two groups, and the ratios of F/G actin. (B) A representative picture of mouse endothelial cells with (Group Ator)/without (Group C) treatment of Ator; both show F-actin in the pattern of lamellipodia, but the intensity of Group Ator was attenuated when compared to that of Group C. Proteins of F-actin and G-actin were evaluated by Western blot representative plot. Compared to Group C, a decrease of F/G actin ratio was observed for Group Ator. \* $p < 0.05$ .

membrane and possess small cytoplasmic domains.<sup>26,27</sup> AP5 in this study was integrin  $\alpha 5 \beta 3$ . Evidence suggested that Ator regulates the activation of integrin, but the relationship between AP5 and Ator was first suggested in our study. Regarding the relationship between Ator and Rac, Fukuyama et al<sup>28</sup> suggested that statins restrain Rac function, which leads to the reduction in osteoblast migration. In addition, Choi et al<sup>29</sup> demonstrated that blocking HMG-CoA reductase pathway in zebrafish and HUVECs results in the inhibition of Rac activity and subsequently reduces the ability of angiogenesis. Recently, Ator has been suggested of having the ability to inhibit the function of Rac-1 induced by Angiotensin II in smooth muscle cells.<sup>30</sup> Taking above all together, Ator has been proven by this study to have the ability to modulate the uPAR-related signaling pathway, and we demonstrated the relationship among Ator, uPAR, AP5, FAK, and Rac in the process of angiogenesis.

Actin is a major cytoskeletal component of endothelial cells. The constant remodeling of actin cytoskeleton into filopodia, lamellipodia, and stress fibers is essential for endothelial cell migration.<sup>31</sup> The protrusion of cytoplasm during cell migration occurs in the form of lamellipodia and filopodia. The filopodia are filamentous membrane projections that contain long parallel actin filaments arranged in tight

bundles. These structures act as sensors of motile stimuli. The lamellipodia are cytoplasmic protrusions that contain a thick cortical network of actin filaments. They are found at the leading edge of migrating cells, allowing their swimming-like motility in the cell. Statins have been suggested to have effects on the remodeling of endothelial cell cytoskeleton.<sup>32,33</sup> Among these studies, Ohkawara et al<sup>34</sup> demonstrated that Ator affects the expression of cell cytoskeleton in endothelial cells. However, there are few studies demonstrating the relationship among lamellipodia, Ator, and angiogenesis. Our study is the first to suggest that Ator decreases F/G actin and expression of F-actin in lamellipodia, which may relate to the attenuation of development of cell migration and tube formation.

Our findings are potentially useful for clinical applications, particularly in the fields of inflammation and cancer diseases. Cumulative evidence indicates that angiogenesis and cytoskeleton transformation are correlated with glomerular diseases. While an imbalance of angiogenesis-related factors is prominent in progression of chronic kidney diseases,<sup>35</sup> dysfunction of podocyte actin cytoskeleton can be linked to proteinuria and glomerular disorders. Although the major portion of this study was on endothelial cells and not podocytes, our results might indicate a new approach for treating glomerular disorders since Ator has been shown clinically beneficial in many glomerular disorders.<sup>36</sup> As previously known, actin cytoskeleton of podocyte foot processes (FPs) is linked to the glomerular basement membrane by 31 integrin,<sup>37</sup> 53 integrin,<sup>38</sup> and  $-/-$ -dystroglycans.<sup>39</sup> Genetic inactivation of 3 or 1 integrin causes podocyte FP effacement and kidney failure in newborn mice, thereby underscoring the critical role of 31 integrin in the development and maintenance of glomerular filtration.<sup>40</sup> Our data demonstrated the close relationship between Ator and AP5, indicating a possible direction for developing AP5 inhibitors with benefits in treating glomerular diseases. While there are only a limited number of IIB 3 and 4 integrin inhibitors in clinical or preclinical phase treatments for cancer and inflammatory disorders, our study suggests a new indication for design and development of potent, selective integrin inhibitors.

In conclusion, a platform of uPARp-luciferase reporter system to screen candidate drugs modulating the expression of uPAR was successfully established. Ator attenuated mEC tube formation and migration, involving uPAR-related factors, AP5, p-FAK, Rac, and reorganization of F-actin cytoskeleton. With the discovery of all-around effect of uPAR modulator, our results may imply the beneficial effect of Ator in glomerular diseases and a new intervention approach in angiogenesis.

#### Acknowledgments

This work was supported by grants from the National Defense Medical Center (C04-06, C06-06, I-33, D101-11-2) and the National Science Council (NSC 100-2314-B-016-020 and NSC 101-2314-B-016-017) and Taipei Medical University (100 TMU-WFH-07), Taiwan, R.O.C. We deeply appreciate Professor Mary Goodwin's efforts in the language support.

## References

- Smith HW, Marshall CJ. Regulation of cell signalling by uPAR. *Nat Rev Mol Cell Biol* 2010;**11**:23–36.
- Bernstein AM, Greenberg RS, Taliana L, Masur SK. Urokinase anchors uPAR to the actin cytoskeleton. *Invest Ophthalmol Vis Sci* 2004;**45**:2967–77.
- Tang H, Kerins DM, Hao Q, Inagami T, Vaughan DE. The urokinase-type plasminogen activator receptor mediates tyrosine phosphorylation of focal adhesion proteins and activation of mitogen-activated protein kinase in cultured endothelial cells. *J Biol Chem* 1998;**273**:18268–72.
- Burgle M, Koppitz M, Riemer C, Kessler H, Konig B, Weidle UH, et al. Inhibition of the interaction of urokinase-type plasminogen activator (uPA) with its receptor (uPAR) by synthetic peptides. *Biological chemistry* 1997;**378**:231–7.
- Rosenberg S. New developments in the urokinase-type plasminogen activator system. *Expert Opin Ther Targets* 2001;**5**:711–22.
- Min HY, Doyle LV, Vitt CR, Zandonella CL, Stratton-Thomas JR, Shuman MA, et al. Urokinase receptor antagonists inhibit angiogenesis and primary tumor growth in syngeneic mice. *Cancer Res* 1996;**56**:2428–33.
- Bauer TW, Liu W, Fan F, Camp ER, Yang A, Somcio RJ, et al. Targeting of urokinase plasminogen activator receptor in human pancreatic carcinoma cells inhibits c-Met- and insulin-like growth factor-I receptor-mediated migration and invasion and orthotopic tumor growth in mice. *Cancer Res* 2005;**65**:7775–81.
- Pillay V, Dass CR, Choong PF. The urokinase plasminogen activator receptor as a gene therapy target for cancer. *Trends Biotechnol* 2007;**25**:33–9.
- Allgayer H. Translational research on u-PAR. *Eur J Cancer* 2010;**46**:1241–51.
- Bugge TH, Suh TT, Flick MJ, Daugherty CC, Rømer J, Solberg H, et al. The receptor for urokinase-type plasminogen activator is not essential for mouse development or fertility. *J Biol Chem* 1995;**270**:1686–94.
- Marek L, Levesse V, Amura C, Zentrich E, Van Putten V, Nemenoff RA, et al. Multiple signaling conduits regulate global differentiation-specific gene expression in PC12 cells. *J Cell Physiol* 2004;**201**:459–69.
- Chen JS, Chang LC, Wu CC, Yeung LK, Lin YF. Involvement of F-actin in chaperonin-containing t-complex 1 beta regulating mouse mesangial cell functions in a glucose-induction cell model. *Exp Diabetes Res* 2011. <http://dx.doi.org/10.1155/2011/565647>.
- Shieh YS, Hung YJ, Hsieh CB, Chen JS, Chou KC, Liu SY. Tumor-associated macrophage correlated with angiogenesis and progression of mucoepidermoid carcinoma of salivary glands. *Ann Surg Oncol* 2009;**16**:751–60.
- Hayot C, Debeir O, Van Ham P, Van Damme M, Kiss R, Decaestecker C. Characterization of the activities of actin-affecting drugs on tumor cell migration. *Toxicol Appl Pharmacol* 2006;**211**:30–40.
- Calebiro D, Nikolaev VO, Gagliani MC, de Filippis T, Dees C, Tacchetti C, et al. Persistent cAMP-signals triggered by internalized G-protein-coupled receptors. *PLoS Biol* 2009;**7**:e1000172.
- Fan F, Wood KV. Bioluminescent assays for high-throughput screening. *Assay Drug Dev Technol* 2007;**5**:127–36.
- Chen Z, Lin L, Huai Q, Huang M. Challenges for drug discovery – a case study of urokinase receptor inhibition. *Comb Chem High Throughput Screen* 2009;**12**:961–7.
- Jamaluddin MS. Aspirin upregulates expression of urokinase type plasminogen activator receptor (uPAR) gene in human colon cancer cells through AP1. *Biochem Biophys Res Commun* 2006;**348**:618–27.
- Lloyd Jr FP, Slivova V, Valachovicova T, Sliva D. Aspirin inhibits highly invasive prostate cancer cells. *Int J Oncol* 2003;**23**:1277–83.
- Hwang JC, Chang LC, Lin YF, Shui HA, Chen JS. Effects of fungal statins on high-glucose-induced mouse mesangial cell hypocontractility may involve filamentous actin, t-complex polypeptide 1 subunit beta, and glucose regulated protein 78. *Transl Res* 2010;**156**:80–90.
- Stach K, Nguyen XD, Lang S, Elmas E, Weiss C, Borggreffe M, et al. Simvastatin and atorvastatin attenuate VCAM-1 and uPAR expression on human endothelial cells and platelet surface expression of CD40 ligand. *Cardiol J* 2012;**19**:20–8.
- Zheng C, Azcutia V, Aikawa E, Figueiredo JL, Croce K, Sonoki H, et al. Statins suppress apolipoprotein CIII-induced vascular endothelial cell activation and monocyte adhesion. *Eur Heart J* 2013;**34**:615–24.
- Ran XZ, Ran X, Zong ZW, Liu DQ, Xiang GM, Su YP, et al. Protective effect of atorvastatin on radiation-induced vascular endothelial cell injury in vitro. *J Radiat Res* 2010;**51**:527–33.
- Urbich C, Dernbach E, Zeiher AM, Dimmeler S. Double-edged role of statins in angiogenesis signaling. *Circ Res* 2002;**90**:737–44.
- Kawakami A, Tanaka A, Nakajima K, Shimokado K, Yoshida M. Atorvastatin attenuates remnant lipoprotein-induced monocyte adhesion to vascular endothelium under flow conditions. *Circ Res* 2002;**91**:263–71.
- Humphries MJ. Integrin structure. *Biochem Soc Trans* 2000;**28**:311–39.
- Nermut MV, Green NM, Eason P, Yamada SS, Yamada KM. Electron microscopy and structural model of human fibronectin receptor. *EMBO J* 1988;**7**:4093–9.
- Fukuyama R, Fujita T, Azuma Y, Hirano A, Nakamura H, Koida M, et al. Statins inhibit osteoblast migration by inhibiting Rac-Akt signaling. *Biochem Biophys Res Commun* 2004;**315**:636–42.
- Choi J, Mouillesseaux K, Wang Z, Fiji HD, Kinderman SS, Otto GW, et al. Aplexone targets the HMG-CoA reductase pathway and differentially regulates arteriovenous angiogenesis. *Development* 2011;**138**:1173–81.
- Shyu KG, Chen SC, Wang BW, Cheng WP, Hung HF. Mechanism of the inhibitory effect of atorvastatin on leptin expression induced by angiotensin II in cultured human coronary artery smooth muscle cells. *Clin Sci (Lond)* 2012;**122**:33–42.
- Lamallice L, Le Boeuf F, Huot J. Endothelial cell migration during angiogenesis. *Circ Res* 2007;**100**:782–94.
- Dunoyer-Geindre S, Fish RJ, Kruihof EK. Regulation of the endothelial plasminogen activator system by fluvastatin. Role of Rho family proteins, actin polymerisation and p38 MAP kinase. *Thromb Haemost* 2011;**105**:461–72.
- Infusino GA, Jacobson JR. Endothelial FAK as a therapeutic target in disease. *Microvasc Res* 2012;**83**:89–96.
- Ohkawara H, Ishibashi T, Sakamoto T, Sugimoto K, Nagata K, Yokoyama K, et al. Thrombin-induced rapid geranylgeranylation of RhoA as an essential process for RhoA activation in endothelial cells. *J Biol Chem* 2005;**280**:10182–8.
- Maeshima Y, Makino H. Angiogenesis and chronic kidney disease. *Fibrogenesis Tissue Repair* 2010;**3**:13.
- Bianchi S, Bigazzi R, Caiazza A, Campese VM. A controlled, prospective study of the effects of atorvastatin on proteinuria and progression of kidney disease. *Am J Kidney Dis* 2003;**41**:565–70.
- Pozzi A, Jarad G, Moeckel GW, Coffa S, Zhang X, Gewin L, et al. Beta1 integrin expression by podocytes is required to maintain glomerular structural integrity. *Dev Biol* 2008;**316**:288–301.
- Schordan S, Schordan E, Endlich K, Endlich N. AlphaV-integrins mediate the mechanoprotective action of osteopontin in podocytes. *Am J Physiol Renal Physiol* 2011;**300**:F119–32.
- Regele HM, Fillipovic E, Langer B, Poczewski H, Kraxberger I, Bittner RE, et al. Glomerular expression of dystroglycans is reduced in minimal change nephrosis but not in focal segmental glomerulosclerosis. *J Am Soc Nephrol* 2000;**11**:403–12.
- Greka A, Mundel P. Cell biology and pathology of podocytes. *Annu Rev Physiol* 2012;**74**:299–323.